

cellular localization of binding partners. When Hel-6 or Hel-v2 were co-expressed with Hel-1 or Ik-1, they were co-localized in the cytoplasm (Fig. 4b, Fig. S2).

Dominant-negative function of ATL-type Helios isoforms against wild-type Helios and Ikaros. We next examined the

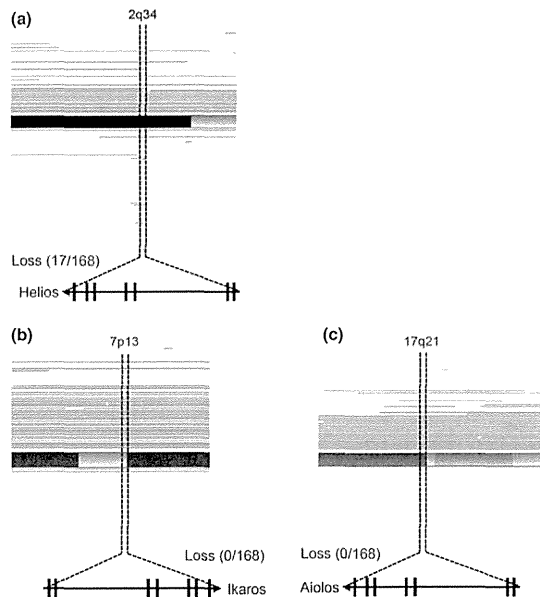


Fig. 2. Genetic abnormalities in *Helios* locus in primary adult T-cell leukemia cells. The results of our copy number analyses³³ (total number, $n = 168$; acute type, $n = 35$; chronic type, $n = 41$; lymphoma type, $n = 44$; smoldering type, $n = 10$; intermediate, $n = 1$; unknown diagnosis, $n = 37$). Tumor-associated deletion of *Helios* region (17/168) was detected (a). No specific genomic losses were observed in *Ikaros* (b) or *Aiolos* loci (c). Recurrent genetic changes are depicted by horizontal lines based on Copy Number Analyser for GeneChip output of the single nucleotide polymorphism array analysis.

functional aspects of these ATL-type Helios isoforms by evaluating their DNA-binding capacities. For EMSA, we used an oligonucleotide probe derived from the promoter region of human *Hes1*, which was a direct target of Ikaros.^{34,35} Ectopically expressed Hel-1 or Ik-1 could bind human *Hes1* promoter DNA (Fig. 5a). Supershift assays confirmed the binding specificity (Fig. 5b). In contrast, all ATL-type Helios isoforms did not show any specific binding to the *Hes1* promoter (Fig. 5a). This impossibility of specific DNA binding of ATL-type Helios was confirmed with another independent DNA probe, IkBS4^{33,36} (data not shown). In addition, it was found in co-expression experiments that Hel-5 had antagonistic effects on the DNA binding capacity of Ik-1 in a dose-dependent manner (Fig. 5c). Reporter assays showed that Hel-1 and Ik-1 suppressed *Hes1* promoter activity. However, ATL-type Helios isoforms did not show any suppressive activity, and actually slightly activated the promoter (Fig. 5d). Furthermore, they also inhibited the suppressive function of Hel-1 and Ik-1 in a dose-dependent manner (Fig. 5e, Fig. S3). These data clearly indicate that ATL-type Helios isoforms are functionally defective because of a DNA binding deficiency and act dominant-negatively in transcriptional suppression induced by Hel-1 or Ik-1. We also confirmed that Hel-2, which lacks only exon 3 and is a major isoform in ATL cells, did not possess suppressive activity against *Hes1* promoter in spite of having binding activity (Fig. 5a,d).

Major ATL-type Helios variant, Hel-5, promotes T cell growth. Given the tumor-suppressive roles of Ikaros family members,¹²⁻¹⁵ it was expected that abnormal splicing of Helios could contribute to T cell leukemogenesis. The mRNA level of Helios was significantly downregulated in ATL-related cell lines compared with that in T-cell lines without HTLV-1 (Fig. 6a, Fig. S4). Moreover, Helios protein was not detected in any ATL-derived or HTLV-1-infected cell lines used in this study (Fig. 6b). In contrast, the expression levels of Ikaros mRNA did not show major differences between HTLV-1-infected and uninfected T-cell lines. Those of Aiolos were low in most cell lines irrespective of HTLV-1 infection (Fig. 6a, Fig. S4). Ikaros protein was detected in all T-cell lines used in this study (Fig. 6b). To elucidate the cellular effects of the expression of dominant-negative ATL-type Helios isoforms in T cells, we established stable Jurkat cells expressing Hel-5 (Fig. 6c). A cell proliferation assay confirmed that Hel-5 expression significantly promoted Jurkat cell proliferation

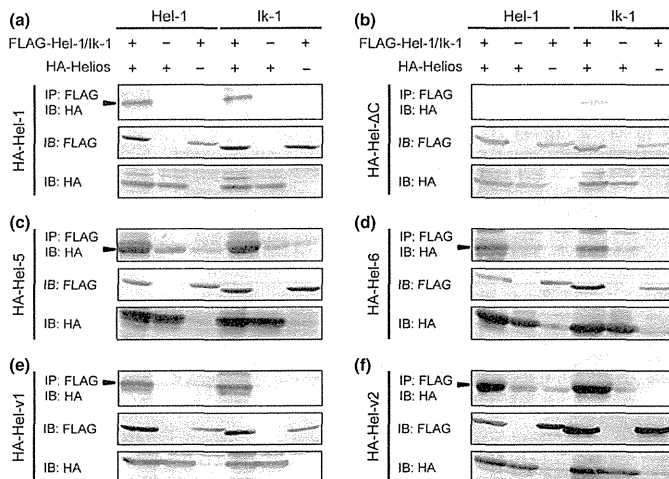


Fig. 3. Dimerization ability of adult T-cell leukemia (ATL)-type Helios isoforms. *In vitro* dimerization assays by co-immunoprecipitation between ATL-type Helios and wild-type Helios or Ikaros proteins. 293T cells were transfected with the indicated combination of expression vectors and subjected to co-immunoprecipitation analyses (top panels). Arrowheads indicate the complex of FLAG and HA-tagged proteins. Middle and bottom panels show the input samples. Hel-1 (a) and Hel-ΔC (b) included as positive and negative controls, respectively. ATL-specific isoforms, Hel-5 (c), Hel-6 (d), Hel-v1 (e), and Hel-v2 (f) were tested. IB, immunoblot; IP, immunoprecipitant.

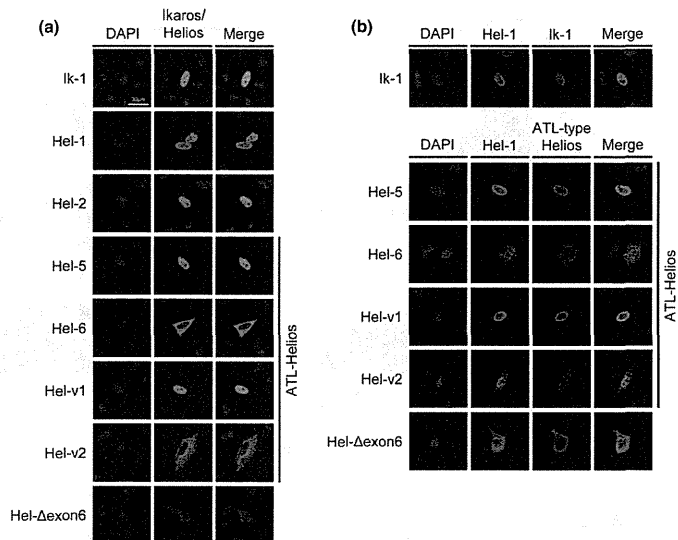


Fig. 4. Subcellular localization of adult T-cell leukemia (ATL)-type Helios isoforms. Immunostaining analyses of Helios and Ikaros proteins. HeLa cells were transfected with each individual expression vector (a) or the indicated combination of expression vectors (b). Each protein was visualized with anti-FLAG (green) or anti-HA antibodies (red). Nuclei were detected by DAPI staining (blue). Colocalization between Ik-1 and ATL-type Helios was shown in Fig. S2. Hel-v1, Hel-variant 1; Hel-v2, Hel-variant 2.

(Fig. 6d). To examine whether the cellular effect of Hel-5 was due to its dominant-negative function against Hel-1 and Ik-1, we carried out further knockdown analyses with specific shRNAs (Fig. 6e). The results showed that knockdown of wild-type Helios or Ikaros led to enhanced cell growth (Fig. 6f), which was consistent with the results of enforced Hel-5 expression. These results collectively suggested that counteraction of Ikaros or Helios by dominant-negative isoforms contributed to T cell growth.

Helios deficiency causes expression of various genes in T cells. We globally searched mRNA expression changes using microarray analysis of Jurkat cells expressing Hel-5 and those of knocked-down Helios or Ikaros (Fig. 7a,b). The results clearly showed differentially expressed gene sets between the transformants and control cells (Fig. 7c). Furthermore, pathway analysis⁽³⁷⁾ of each upregulated gene set identified activation of several signaling cascades. In particular, we focused on six common pathways identified in both Hel-5 transduced and Helios or Ikaros knocked-down Jurkat cells (Fig. 7d). These pathways are important for various T cell regulations, for example, cell growth, apoptosis resistance, and migration activity. Among these pathways, it has not been reported that the shingosine-1-phosphate (S1P) pathway is regulated by the Ikaros family. We confirmed overexpressed *S1PR1* and *S1PR3*, which are critical receptors for the activation of the S1P pathway, in manipulated Jurkat samples (Fig. 7e).

Discussion

In the present study, on the basis of the integrated analysis of ATL cells using our biomaterial bank in Japan, we revealed a novel molecular characteristic of ATL cells, which is a profound abnormality in the expression of Helios. The abnormal alternative splicing and, in some cases, loss of Helios expression appear to be a part of the basis for advantageous cell growth and survival in ATL cells. We also showed the tumor-suppressive function and target genes, as well as pathways of Helios, in mature human T cells.

Characterization of Ikaros family members revealed profound abnormalities in Helios expression in ATL cells: (i)

biased and increased expression of alternatively spliced variants; (ii) suppression of Hel-1 expression; (iii) lack of Helios expression in some cases; and (iv) frequent genomic defects of the *Helios* locus. Our results also revealed that alternatively spliced Helios variants are expressed in PBMCs of HTLV-1 carriers, suggesting that the abnormal splicing of Helios may occur in HTLV-1-infected cells at the carrier state until progression to leukemia development. However, the genomic deletions appear to be one of the important genetic events during the latter stages of leukemia development, as they were observed only in aggressive subtypes of ATL.

The structural characteristics of the ATL-type Helios variants involve a selective lack of one or more zinc fingers in the N-terminal domain. The results of this study indicated that these variant proteins lost DNA binding activity, whereas the capacity of dimerization was preserved. Therefore, these variant proteins hindered transcriptional activities of Ikaros family proteins, showing dominant-negative effects. In addition, a part of ATL-type Helios isoform, which lacks exon 6, is linked to abnormal localization of wild-type Helios and Ikaros. We confirmed that Helios isoforms lacking exon 6 were overexpressed in primary ATL cells (Fig. S5). Interestingly, Hel-2 has reduced transcriptional suppressive activity compared with Hel-1, although it can bind to the target sequence as well as Hel-1. This is similar to a previous report,⁽³⁶⁾ which noted that the activity of mouse Ik-2 protein for the reporter gene was remarkably lower than that of Ik-1, whereas the binding affinities of Ik-1 and Ik-2 were similar. The exon 3 skip occurred more frequently in ATL cells, compared to PBMCs from normal volunteers (Fig. S6). These results collectively indicate that all abnormalities of Helios expression, including loss of or decreased Hel-1 expression and upregulated Hel-2 and ATL-type Helios, result in abrogation of Ikaros family functions in ATL cells.

We also confirmed that *Hes1*, a target gene of the Notch pathway, is one of the targets of Helios as well as Ikaros.^(34,35) A recent study reported that activated Notch signaling may be important to ATL pathogenesis and that *Hes1* is upregulated in ATL cells.⁽³⁸⁾ Thus, we examined expression levels of *Hes1* mRNA by quantitative RT-PCR and confirmed the

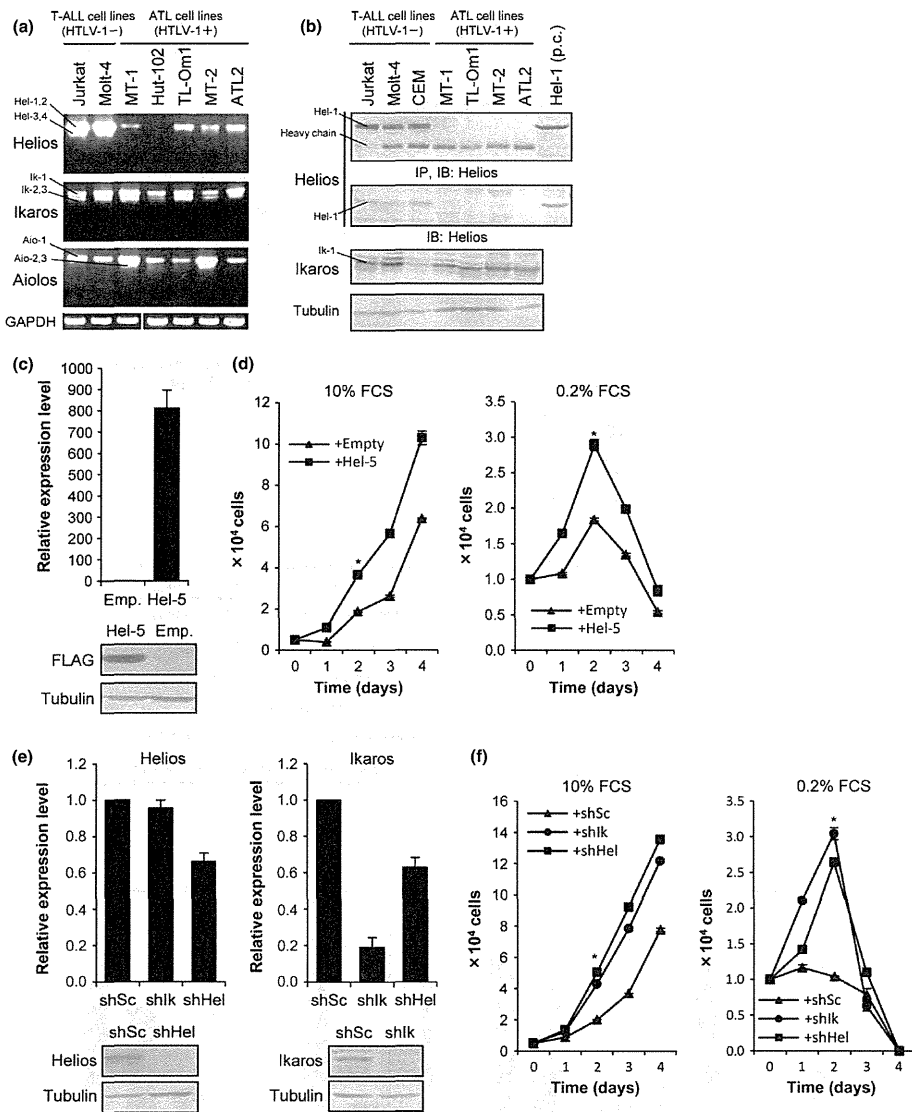


Fig. 6. Hel-5 functions in T cell growth and survival. (a) Expression patterns and levels of Ikaros family genes in various cell lines examined by RT-PCR. ATL, adult T-cell leukemia; T-ALL, acute T lymphoblastic leukemia. (b) Results of immunoblotting analyses of the immunoprecipitants (top panel) and cell lysates (lower panels). Positive control (p.c.), Hel-1 transfectant. IB, immunoblot; IP, immunoprecipitant. (c) Establishment of Jurkat cells stably expressing Hel-5. The Hel-5 level was quantified by quantitative RT-PCR (top, $n = 3$, mean \pm SD) and immunoblotting (bottom). (d) Cell proliferation analysis of control cells (▲) and Hel-5-expressing Jurkat cells (■) under two FCS conditions ($n = 3$, mean \pm SD). Statistical significance was observed ($*P < 0.01$, Student's *t*-test). (e) Knockdown analyses of Helios or Ikaros in Jurkat cells. The Helios and Ikaros levels were evaluated by quantitative RT-PCR (top, $n = 3$, mean \pm SD) and immunoblotting (bottom), respectively. (f) Cell proliferation curves of scrambled shRNA (shSc) cells (▲), shIkaros (shIk) cells (●), and shHelios (shHel) cells (■) were examined in two FBS conditions ($n = 3$, mean \pm SD; $*P < 0.01$).

roles in regulation of the immune system, apoptosis, cell cycle, and migration of lymphocytes.^(40–42) Recently, activation of the S1P pathway in various diseases, including leukemia, has been reported, and the therapeutic potential of S1PR1 inhibitors was suggested.⁽⁴²⁾ Studies of functional roles of S1P pathway activation in ATL cells are now underway in our laboratory.

In conclusion, our present study revealed a novel aspect of molecular abnormalities in ATL cells: a profound deregulation in Helios expression, which appears to play an important role in T-cell proliferation. Our experimental approaches also imply that, in addition to genetic and epigenetic abnormalities, ATL shows abnormal splicing, which has been observed in various human diseases including cancers.^(43–45)

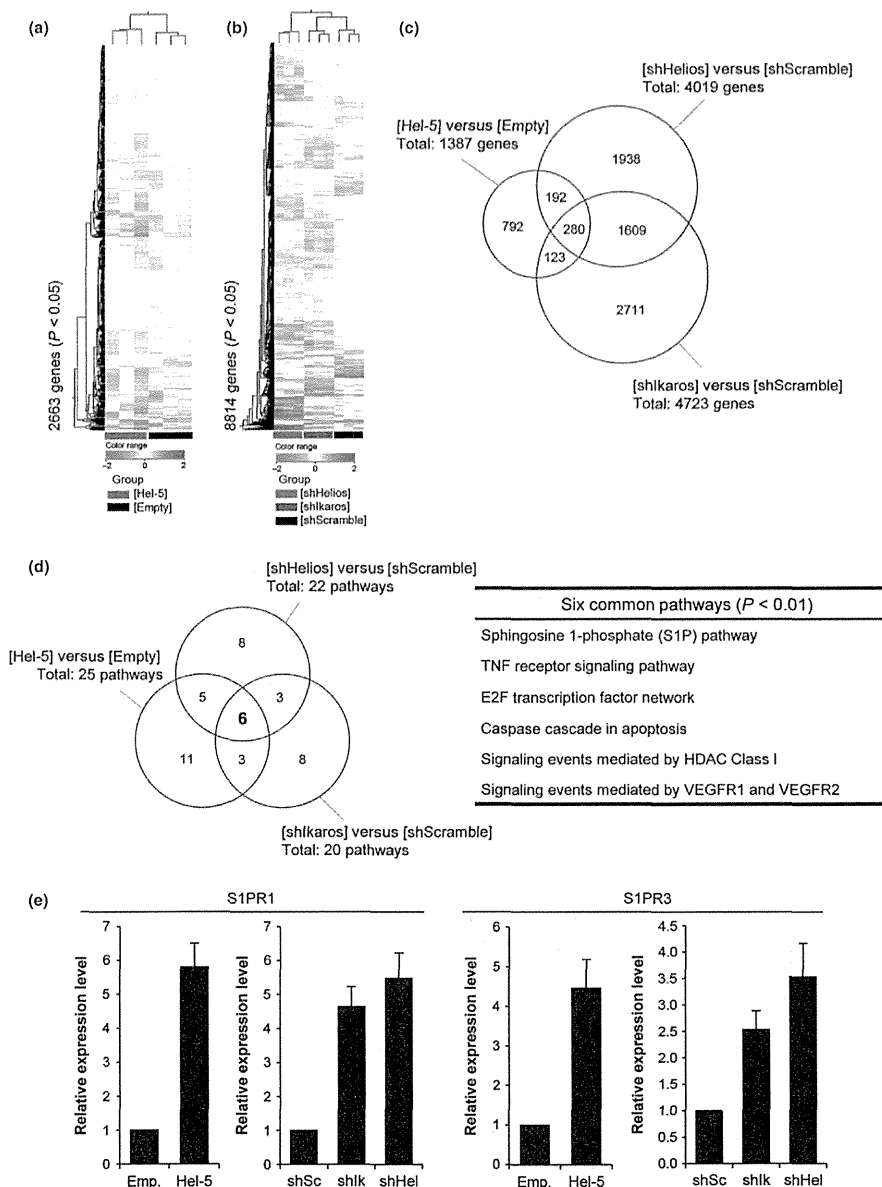


Fig. 7. Comprehensive search for Helios target genes by microarray analysis. (a,b) Gene expression analysis of Jurkat stable cells. The gene expression patterns of Jurkat cells expressing Hel-5 ($n = 3$), shkarnos ($n = 3$), and shHelios ($n = 3$) were comprehensively analyzed by microarray technique. The obtained 2D hierarchical clusters and Pearson's correlation between the cells expressing Hel-5 or not (a) and the cells introducing shHel, shlk, or shSc (b). (c) Venn diagram of differential gene expression pattern in the Jurkat sublines. The each differential expression gene set (5-fold changes, $P < 1 \times 10^{-5}$) was compared. (d) Venn diagram depicting the overlap between the outputs of pathway analysis in Jurkat sublines. The analysis was based on the NCI-Nature Pathway Interaction Database.⁽³⁷⁾ Each differential pathway set (t-test, $P < 0.01$) was compared and the common pathways listed. (e) Results of quantitative RT-PCR of shingosine-1-phosphate receptor 1 (S1PR1) and receptor 3 (S1PR3) in Jurkat sublines ($n = 3$, mean \pm SD). HDAC, histone deacetylase; VEGFR, vascular endothelial growth factor receptor.

Acknowledgments

We thank Mr. M. Nakashima and Ms. T. Akashi for support and maintenance of the Joint Study on Prognostic Factors of ATL Development. This

work is supported by JSPS KAKENHI Grant Numbers 24790436 (M.Y.), 23390250 (T.W.), 23659484 (T.W.), 23 6291 (S.A.), NEXT KAKENHI Grant Number 221S0001 (T.W.), and a Grant-in-Aid from the Ministry of Health, Labor and Welfare of Japan H24-G-004 (M.Y. and T.W.).

Disclosure Statement

The authors have no conflict of interest.

References

- 1 Yamaguchi K, Watanabe T. Human T lymphotropic virus type-I and adult T-cell leukemia in Japan. *Int J Hematol* 2002; **76**: 240–45.
- 2 Iwanaga M, Watanabe T, Utsunomiya A *et al*. Human T-cell leukemia virus type I (HTLV-I) proviral load and disease progression in asymptomatic HTLV-I carriers: a nationwide prospective study in Japan. *Blood* 2010; **116**: 1211–19.
- 3 Yamagishi M, Nakano K, Miyake A *et al*. Polycomb-mediated loss of miR-31 activates NIK-dependent NF- κ B pathway in adult T cell leukemia and other cancers. *Cancer Cell* 2012; **21**: 121–35.
- 4 Yamagishi M, Watanabe T. Molecular hallmarks of adult T cell leukemia. *Front Microbiol* 2012; **3**: 334.
- 5 Lo K, Landau NR, Smale ST. LyF-1, a transcriptional regulator that interacts with a novel class of promoters for lymphocyte-specific genes. *Mol Cell Biol* 1991; **11**: 5229–43.
- 6 Georgopoulos K, Moore DD, Derfler B. Ikaros, an early lymphoid-specific transcription factor and a putative mediator for T cell commitment. *Science* 1992; **258**: 808–12.
- 7 Hahn K, Ernst P, Lo K, Kim GS, Turck C, Smale ST. The lymphoid transcription factor LyF-1 is encoded by specific, alternatively spliced mRNAs derived from the Ikaros gene. *Mol Cell Biol* 1994; **14**: 7111–23.
- 8 Sun L, Liu A. Zinc finger-mediated protein interactions modulate Ikaros activity, a molecular control of lymphocyte development. *EMBO J* 1996; **15**: 5358–69.
- 9 Morgan B, Sun L, Avitahl N *et al*. Aiolos, a lymphoid restricted transcription factor that interacts with Ikaros to regulate lymphocyte differentiation. *EMBO J* 1997; **16**: 2004–13.
- 10 Kelley CM, Ikeda T, Koipally J *et al*. Helios, a novel dimerization partner of Ikaros expressed in the earliest hematopoietic progenitors. *Curr Biol* 1998; **8**: 508–15.
- 11 Cobb BS, McCarty AS, Brown KE *et al*. Helios, a T cell-restricted Ikaros family member that quantitatively associates with Ikaros at centromeric heterochromatin. *Genes Dev* 1998; **12**: 782–96.
- 12 Winandy S, Wu P, Georgopoulos K. A dominant mutation in the Ikaros gene leads to rapid development of leukemia and lymphoma. *Cell* 1995; **83**: 289–99.
- 13 Wang JH, Nichogiannopoulou A, Wu L *et al*. Selective defects in the development of the fetal and adult lymphoid system in mice with an Ikaros null mutation. *Immunity* 1996; **5**: 537–49.
- 14 Wang JH, Avitahl N, Cariappa A *et al*. Aiolos regulates B cell activation and maturation to effector state. *Immunity* 1998; **9**: 543–53.
- 15 Zhang Z, Swindle CS, Bates JT, Ko R, Cotta CV, Klug CA. Expression of a non-DNA-binding isoform of Helios induces T-cell lymphoma in mice. *Blood* 2007; **109**: 2190–7.
- 16 Sun L, Crotty ML, Sensel M *et al*. Expression of dominant-negative Ikaros isoforms in T-cell acute lymphoblastic leukemia. *Clin Cancer Res* 1999; **5**: 2112–20.
- 17 Nakase K, Ishimaru F, Avitahl N *et al*. Dominant negative isoform of the Ikaros gene in patients with adult B-cell acute lymphoblastic leukemia. *Cancer Res* 2000; **60**: 062–4065.
- 18 Takanashi M, Yagi T, Imamura T *et al*. Expression of the Ikaros gene family in childhood acute lymphoblastic leukaemia. *Br J Haematol* 2002; **117**: 525–30.
- 19 Nishii K, Katayama N, Miwa H. Non-DNA-binding Ikaros isoform gene expressed in adult B-precursor acute lymphoblastic leukemia. *Leukemia* 2002; **16**: 1285–92.
- 20 Tonnelie C, Imbert M-C, Sainy D, Granjeaud S, N'Guyen C, Chabannon C. Overexpression of dominant-negative Ikaros 6 protein is restricted to a subset of B common adult acute lymphoblastic leukemias that express high levels of the CD34 antigen. *Hematol J* 2003; **4**: 104–9.
- 21 Klein F, Feldhahn N, Herzog S *et al*. BCR-ABL1 induces aberrant splicing of IKAROS and lineage infidelity in pre-B lymphoblastic leukemia cells. *Oncogene* 2006; **25**: 1118–24.
- 22 Zhou F, Mei H, Jin R, Li X, Chen X. Expression of ikaros isoform 6 in chinese children with acute lymphoblastic leukemia. *J Pediatr Hematol Oncol* 2011; **33**: 429–32.
- 23 Mullighan CG, Miller CB, Radtke I *et al*. BCR-ABL1 lymphoblastic leukaemia is characterized by the deletion of Ikaros. *Nature* 2008; **453**: 110–14.
- 24 Kano G, Morimoto A, Takanashi M *et al*. Ikaros dominant negative isoform (Ik6) induces IL-3-independent survival of murine pro-B lymphocytes by activating JAK-STAT and up-regulating Bcl-x1 levels. *Leuk Lymphoma* 2008; **49**: 965–73.
- 25 Iacobucci I, Lonetti A, Messa F *et al*. Expression of spliced oncogenic Ikaros isoforms in Philadelphia-positive acute lymphoblastic leukemia patients treated with tyrosine kinase inhibitors: implications for a new mechanism of resistance. *Blood* 2008; **112**: 3847–55.
- 26 Mullighan CG, Su X, Zhang J *et al*. Deletion of IKZF1 and prognosis in acute lymphoblastic leukemia. *N Engl J Med* 2009; **360**: 470–80.
- 27 Kuiper RP, Waanders E, van der Velden VHJ *et al*. IKZF1 deletions predict relapse in uniformly treated pediatric precursor B-ALL. *Leukemia* 2010; **24**: 1258–64.
- 28 Nakase K, Ishimaru F, Fujii K *et al*. Overexpression of novel short isoforms of Helios in a patient with T-cell acute lymphoblastic leukemia. *Exp Hematol* 2002; **30**: 313–17.
- 29 Fujii K, Ishimaru F, Tabayashi T *et al*. Over-expression of short isoforms of Helios in patients with adult T-cell leukaemia/lymphoma. *Br J Haematol* 2003; **120**: 986–9.
- 30 Fujiwara SI, Yamashita Y, Nakamura N *et al*. High-resolution analysis of chromosome copy number alterations in angioimmunoblastic T-cell lymphoma and peripheral T-cell lymphoma, unspecified, with single nucleotide polymorphism-typing microarrays. *Leukemia* 2008; **22**: 1891–8.
- 31 Fujimoto R, Ozawa T, Itoyama T, Sadamori N, Kurosawa N, Isobe M. HELIOS-BCL11B fusion gene involvement in a t(2;14)(q34;q32) in an adult T-cell leukemia patient. *Cancer Genet* 2012; **205**: 356–64.
- 32 Shimoyama M. Diagnostic criteria and classification of clinical subtypes of adult T-cell leukaemia-lymphoma. A report from the Lymphoma Study Group (1984–87). *Br J Haematol* 1991; **79**: 428–37.
- 33 Tabayashi T, Ishimaru F, Takata M *et al*. Characterization of the short isoform of Helios overexpressed in patients with T-cell malignancies. *Cancer Sci* 2007; **98**: 182–8.
- 34 Kathrein KL, Chari S, Winandy S. Ikaros directly represses the notch target gene Hes1 in a leukemia T cell line: implications for CD4 regulation. *J Biol Chem* 2008; **283**: 10476–84.
- 35 Kleinmann E, Geimer Le Lay AS, Sellars M, Kastner P, Chan S. Ikaros represses the transcriptional response to Notch signaling in T-cell development. *Mol Cell Biol* 2008; **28**: 7465–75.
- 36 Molnár A, Georgopoulos K. The Ikaros gene encodes a family of functionally diverse zinc finger DNA-binding proteins. *Mol Cell Biol* 1994; **14**: 8292–303.
- 37 Schaefer CF, Anthony K, Krupa S *et al*. PID: the pathway interaction database. *Nucleic Acids Res* 2009; **37**: D674–9.
- 38 Pancewicz J, Taylor JM, Datta A. Notch signaling contributes to proliferation and tumor formation of human T-cell leukemia virus type 1-associated adult T-cell leukemia. *Proc Natl Acad Sci USA* 2010; **107**: 16619–24.
- 39 Murata K, Hattori M, Hirai N *et al*. Hes1 directly controls cell proliferation through the transcriptional repression of p27Kip1. *Mol Cell Biol* 2005; **25**: 4262–71.
- 40 Maeda Y, Seki N, Sato N, Sugahara K, Chiba K. Sphingosine 1-phosphate receptor type 1 regulates egress of mature T cells from mouse bone marrow. *Int Immunol* 2010; **22**: 515–25.
- 41 Spiegel S, Milstien S. The outs and the ins of sphingosine-1-phosphate in immunity. *Nat Rev Immunol* 2011; **11**: 403–15.
- 42 Maceyka M, Harikumar KB, Milstien S, Spiegel S. Sphingosine-1-phosphate signaling and its role in disease. *Trends Cell Biol* 2012; **22**: 50–60.
- 43 Ghigna C, Valacca C, Biamonti G. Alternative splicing and tumor progression. *Curr Genomics* 2008; **9**: 556–70.
- 44 David CJ, Manley JL. Alternative pre-mRNA splicing regulation in cancer: pathways and programs unhinged. *Genes Dev* 2010; **24**: 2343–64.
- 45 Blair CA, Zi X. Potential molecular targeting of splice variants for cancer treatment. *Indian J Exp Biol* 2011; **49**: 836–9.

Supporting Information

Additional Supporting Information may be found in the online version of this article:

Fig. S1. Deregulated expression of Ikaros family genes in primary adult T-cell leukemia cells.

Effects of riboflavin and ultraviolet light treatment on platelet thrombus formation on collagen via integrin α IIb β 3 activation

Chikahiro Terada, Junpei Mori, Hitoshi Okazaki, Masahiro Satake, and Kenji Tadokoro

BACKGROUND: The adoption of pathogen reduction technology (PRT) is considered for the implementation of safer platelet (PLT) transfusion. However, the effects of PRT treatment on PLT thrombus formation under blood flow have not yet been fully clarified.

STUDY DESIGN AND METHODS: Leukoreduced PLT concentrates (PCs) obtained by plateletpheresis were treated with riboflavin and ultraviolet light (Mirasol PRT). PC samples were passed through a column filled with collagen-coated beads at a fixed shear rate after 1, 3, and 5 days of storage. The thrombus formation ability was evaluated by measuring collagen column retention rate. The change in the activation state of integrin α IIb β 3 on PLTs during storage was examined by flow cytometry.

RESULTS: The retention rate of the PRT-treated PLTs was significantly higher than that of the control PLTs on the day of treatment and decreased with storage but remained higher than those of the control during storage. This modification did not correlate with the total α IIb β 3 or fibrinogen binding on the PLTs but correlated significantly with PAC-1 binding. Mn²⁺-induced α IIb β 3 activation also fully restored the retention rate in the Day 5 PRT-treated PLTs along with the increase in PAC-1 binding.

CONCLUSION: Riboflavin-based PRT treatment of PCs leads to the enhancement of thrombus formation on collagen, which is related to the activation status of α IIb β 3, which does not bind to fibrinogen but binds to PAC-1. The impact of this finding on the hemostatic or even thrombogenic potential in vivo must await clinical evaluation.

The safety of blood transfusion has been improved markedly owing to advances in blood donor selection and blood testing. Concerns still exist, however, because of a relatively high incidence of bacterial contamination of platelet (PLT) products and the possible risk of transfusion-transmitted infection by emerging pathogens.¹ Therefore, the adoption of pathogen reduction technologies (PRTs) that broadly and nonspecifically inactivate pathogens is being considered in many countries for the implementation of safer PLT transfusions. Current PRTs are based on inactivation methods using ultraviolet (UV) light irradiation with or without a photosensitizing agent against pathogen nucleic acids.² The Mirasol PRT system (Terumo BCT, Tokyo, Japan) uses UV light (265-370 nm) and a photosensitizing agent, riboflavin.³ It is currently approved in some European countries for the treatment of PLT concentrates (PCs) in plasma or additive solution.⁴

Although PRT treatment enhances the safety of PCs, there are concerns about the decrease in product quality.⁵ In vitro quality measurements of PCs during the storage period revealed a contribution of the PRT treatment to the PLT storage lesion when compared with the untreated controls. A decrease in pH, increase in P-selectin expression level, and decline in swirling were observed in PRT-treated PLTs.⁶ In addition, the enhancement of glucose

ABBREVIATIONS: AP = apheresis; PC(s) = platelet concentrate(s); PRP = platelet-rich plasma; PRT(s) = pathogen reduction technology(-ies); TRAP = thrombin receptor-activating peptide.

From the Department of Research and Development, Central Blood Institute, Japanese Red Cross Society, Tokyo, Japan.

Address reprint requests to: Chikahiro Terada, Department of Research and Development, Central Blood Institute, Japanese Red Cross Society, 2-1-67 Tatsumi, Koto-ku, Tokyo 135-8521, Japan; e-mail: c-terada@jrc.or.jp.

Received for publication May 1, 2013; revision received November 29, 2013, and accepted December 2, 2013.

doi: 10.1111/trf.12566

© 2014 AABB

TRANSFUSION **,**,**,**

consumption and lactate production and the presence of mitochondrial dysregulation in PRT-treated PLTs were reported.^{7,8} There have been various reports on the alteration of PLT functions caused by PRT treatment. The PLT aggregation in response to collagen and thrombin receptor-activating peptide (TRAP) was reported to be lesser in PRT-treated PLTs than in untreated control PLTs.⁹ On the other hand, the adhesion of PRT-treated PLTs to assay plates was shown to be greater than that of control PLTs by the results of thrombus formation assay using Impact-R (DiaMed, Cressier sur Morat, Switzerland), which reflects the PLT ability for adhesion and aggregation associated with a shear stress caused by blood flow.¹⁰ Moreover, using a perfusion model with rabbit aorta segments, the thrombus formation after storage was better maintained in PRT-treated PLTs than in control PLTs.¹¹ It seems that results in regard to the effects of PRT treatment on PLT functions vary depending on the assay methods used. In single-blind crossover studies, *in vivo* recovery and survival of PRT-treated PCs were reduced compared with those of untreated control units, as evidenced by reduced corrected count increment.^{12,13} However, the results of a recent pilot study of PLT function in PRT-treated PLTs isolated from the circulation of patients after transfusion have suggested that these circulating cells may elicit hemostatic responses comparable to those in untreated PLTs.¹⁴ To develop strategies that minimize the negative effects of PRT, it is necessary to determine the mechanisms by which PLTs are damaged.

In this study, we prepared columns filled with collagen-coated beads and performed a thrombus formation assay to clarify the effects of PRT treatment on PLT functions. In our collagen column method, thrombus formation on the solid-phase collagen similar to that observed in the damaged vascular subendothelium was assayed at a constant shear rate. This method better reflects physiologic conditions than PLT aggregometry, in which PLTs are simply stirred in the presence of agonists. Moreover, the collagen column method utilizes PLT-rich plasma (PRP), which is different from other methods using a flow chamber or Impact-R that require reconstituted blood or whole blood samples. Using the collagen column method, we determined the effects of PRT treatment on PLT thrombus formation and examined the mechanism underlying the effects.

MATERIALS AND METHODS

Materials

Common chemicals were purchased from Sigma-Aldrich (St Louis, MO) or Wako Pure Chemicals (Osaka, Japan). Copolymer plastic beads (165 μ m in diameter on average) coated with porcine Type I collagen were purchased from ISK (Tokyo, Japan). A monoclonal Alexa Fluor 488-conjugated CD41 antibody (Clone MEM-06) was pur-

chased from EXBIO (Prague, Czech Republic). A monoclonal fluorescein isothiocyanate (FITC)-conjugated PAC-1 antibody was purchased from BD Biosciences (San Jose, CA). A monoclonal phycoerythrin (PE)-cyanin 5.1 (PC5)-conjugated anti-CD41 antibody (Clone P2) was purchased from Beckman Coulter (Fullerton, CA). Polyclonal FITC-conjugated anti-human fibrinogen antibodies were purchased from Binding Site (PF056, Birmingham, UK) and Agrisera (IMS09-038-335, Vannas, Sweden).

Preparation of PCs

Informed consent was obtained from all healthy volunteers before apheresis (AP) donation. Leukoreduced AP-PCs (volume of 230 ± 16 mL and yield of $3.4 \times 10^{11} \pm 0.8 \times 10^{11}$ PLTs/bag) were collected using automated blood collection systems (Trima Accel, Terumo BCT; or CCS, Haemonetics, Braintree, MA).

PRT treatment

The Mirasol PRT treatment ($n = 32$, blood group composition: A, 12; B, 3; O, 17) was performed on Day 1 postcollection as described elsewhere.^{6,8,15} Briefly, after the addition of 35 mL of riboflavin solution to an AP-PC bag at a final concentration of 50 μ mol/L, the bag was exposed to UV light at a dose of 6.24 J/mL (265-370 nm) and allowed to stand for 30 minutes before placement on a flatbed agitator running at 55 agitations per minute. To the untreated control bag ($n = 17$, blood group composition: A, 4; B, 1; O, 12), 35 mL of a 0.9% saline solution was added. All PCs were kept at 20 to 24°C on the flatbed agitator for 5 days. All PLT samples were taken from bags, under sterile conditions, at 2 hours after PRT treatment and after 3 and 5 days of storage.

Thrombus formation assay and fluorescence microscopy

Collagen columns were prepared by filling silicon tubes (4-mm outer diameter, 2-mm inner diameter, and 50-mm length) with copolymer plastic beads coated with porcine Type I collagen using dry air (9 mL/min, 10 min) from an air compressor. Thus-prepared columns were set in an incubator at 37°C. PRP (30×10^{10} PLTs/L) prepared from PCs was incubated at 37°C for 10 minutes, and 0.5 mL of PRP was then passed through the columns at a shear rate of 750 per second by aspirating with a syringe pump (Fig. 1). This shear rate was calculated on the basis of previous reports.^{16,17}

Retention rates obtained from PLT counts before and after the passage of PRP through the columns were used as indices of thrombus formation. All of the PRP samples before and after passage through the columns were

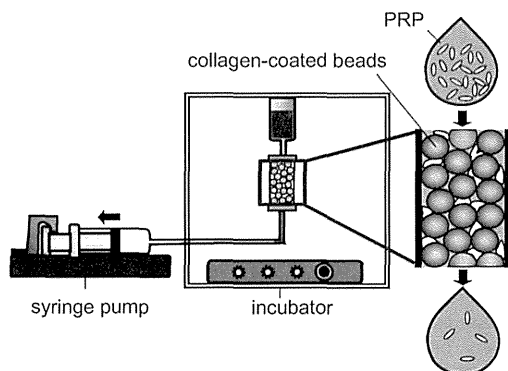


Fig. 1. Schematic diagram of collagen column system used for thrombus formation assay.

collected into plastic tubes containing ethylenediaminetetraacetic acid (5 mmol/L), and PLT count was determined using an automatic blood cell counter (XS-800i, Sysmex, Kobe, Japan). PLT retention rate (%) was calculated as follows: [(total PLT count before passing through the column) - (total PLT count after passing through the column)] / (total PLT count before passing through the column) \times 100.

In one experiment, beads were taken from the columns through which PRP was passed and fixed with 1% paraformaldehyde phosphate-buffered saline (PBS) for 1 hour. The beads were then fluorescently stained with an Alexa Fluor 488-conjugated anti-CD41. The fluorescent images of PLT thrombus formed on the beads were observed by fluorescence microscopy (IX-71, Olympus, Tokyo, Japan) at 40 \times magnification.

Flow cytometry

Total α IIb β 3 level was measured on the basis of the level of binding of the anti-CD41 (P2) to the α IIb β 3 complex. The state of α IIb β 3 activation was evaluated on the basis of PAC-1 binding or fibrinogen binding. PLT samples were incubated with an FITC-conjugated PAC-1 antibody or FITC-conjugated polyclonal anti-human fibrinogen antibodies and a PE-cyanin 5.1-conjugated anti-CD41 for 20 minutes at room temperature. Isotype control antibodies were also included as controls. The samples were fixed with 1% paraformaldehyde PBS and analyzed by flow cytometry using the accompanying software (Cytomics FC500 and CXP software Version 2, respectively, Beckman Coulter, Miami, FL). Fluorescence data from 10,000 PLT events were collected in the logarithmic mode.

To examine the maximum binding of fibrinogen to PLTs, PLT samples, either PRT treated or untreated, were stimulated with 100 μ mol/L TRAP for 5 minutes and

stained with an FITC-conjugated anti-fibrinogen antibody and then subjected to flow cytometry analysis.

Mn²⁺ treatment

To clarify the effect of α IIb β 3 activation on thrombus formation, in some experiments, PRP samples were incubated with 1 mmol/L MnCl₂ as the activating agent at 37°C for 5 minutes before the thrombus formation assay and flow cytometry. As previously shown by others, this concentration of Mn²⁺ can fully activate α IIb β 3.^{18,19}

Statistical analysis

Results are presented as mean \pm SD. The t test was conducted with p values of not more than 0.05 indicating a significant difference. Correlations were determined using Spearman's rank correlation method. A correlation coefficient of more than 0.75 between methods was considered to indicate a good to excellent relationship. A correlation coefficient from 0 to 0.25 indicated a poor or no relationship.²⁰

RESULTS

Effects of PRT treatment on PLT thrombus formation

We measured retention rate as an index of thrombus formation by the collagen column method. The retention rate of the PRT-treated PLTs on the day of treatment (Day 1) was 97.3 \pm 6.1%, which was significantly higher than that of the control PLTs, 39.5 \pm 21.7%, by more than twofold (Fig. 2A). Riboflavin alone without UV radiation did not increase the retention rate (46.1 \pm 23.3%, n = 7, data not shown). We also observed the fluorescent images of PLT thrombi formed on the collagen-coated beads taken from the columns through which PRP passed. There were more PLTs and larger thrombi that covered multiple beads through which the Day 1 PRT-treated PLTs passed than on the beads through which the control PLTs passed (Fig. 2B). The retention rate of the PRT-treated PLTs was highest on Day 1 and decreased with storage period. The retention rate of the PRT-treated PLTs was significantly higher than that of the control PLTs throughout the storage period (Fig. 2A). These findings showed that PRT treatment enhanced the thrombus formation of the PLTs on collagen and that the thrombus formation was well maintained during the storage period.

Effects of PRT treatment on α IIb β 3

α IIb β 3 molecules on the PLT surface play a crucial role in thrombus formation. We examined the effects of PRT treatment on α IIb β 3 using the P2 antibody, which

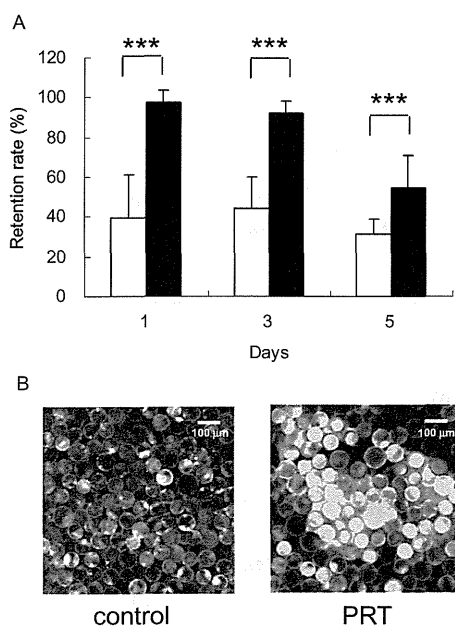


Fig. 2. Effects of PRT treatment on PLT thrombus formation. (A) Thrombus formation by collagen column method: control (□), PRT treated (■). (B) Typical fluorescent image of thrombus on collagen-coated beads through which Day 1 PLTs passed: (left) control; (right) PRT treated. Thrombus formation was determined on the basis of retention rate (%) presented as mean \pm SD. $n = 17$ (□); $n = 32$ (■). *** $p < 0.001$.

recognizes the α Ib β 3 complex; the PAC-1 antibody, which recognizes conformational changes caused by α Ib β 3 activation; and the anti-fibrinogen antibody. There was no significant difference in the total α Ib β 3 level between the PRT-treated PLTs and the control PLTs on Day 1 (Fig. 3A). From the third day of storage, the total α Ib β 3 level on the PRT-treated PLTs was significantly higher than that on the control PLTs. The PAC-1 binding on the PRT-treated PLTs was significantly higher than that on the control PLTs ($85.3 \pm 9.4\%$ vs. $10.7 \pm 7.1\%$) on Day 1 (Fig. 3B) and decreased with storage time while maintaining a higher level than that on the control PLTs throughout the storage period. Using PF056, the level of fibrinogen binding on the PRT-treated PLTs (5.26 ± 1.34) was significantly higher than that on the control PLTs (4.08 ± 0.61) on Day 1 (Fig. 3C). However, it gradually increased with storage time compared with the control, which is in marked contrast to PAC-1 binding which shows a decreasing trend with storage time. The increasing trend of fibrinogen

binding was confirmed with the other polyclonal antibodies specific for fibrinogen (data not shown). When the Day 1 PRT-treated PLTs were stimulated by TRAP, fibrinogen binding level markedly increased by 10.6- and 7.9-fold in terms of mean fluorescence intensity for control and PRT-treated PLTs, respectively ($n = 4$, data not shown), indicating that the fibrinogen binding is only partial although it increases with storage time. These findings show that PRT treatment immediately activated α Ib β 3 and sustained α Ib β 3 activation during the storage period; however, the sustained α Ib β 3 activation did not correspond to the increasing trend of total α Ib β 3 level and fibrinogen binding level.

Correlation between thrombus formation and activation of α Ib β 3

We compared the retention rate measured by the collagen column method with the activation marker measured by flow cytometry for all the PRT-treated and control PLT samples to determine the correlation between thrombus formation and α Ib β 3 activation ($n = 49$; Table 1). There were no correlations between retention rate and total α Ib β 3 level (P2 binding) or fibrinogen binding level (Spearman $r < 0.25$). However, there was a significant correlation between retention rate and α Ib β 3 activation (PAC-1 binding; Spearman $r = 0.840$, $p < 0.001$). These findings suggest that α Ib β 3 activation affected the thrombus formation as verified by the collagen column method, whereas the thrombus formation did not correlate with the total α Ib β 3 level or fibrinogen binding level.

Effects of Mn^{2+} on α Ib β 3 and thrombus formation

We measured the retention rate and PAC-1 binding level in the Day 5 PRT-treated PLTs and control PLTs after incubation with 1 mmol/L $MnCl_2$ at 37°C for 5 minutes to determine whether thrombus formation is restored by the reactivation of α Ib β 3. Mn^{2+} directly activates α Ib β 3 extracellularly without being mediated by signals from inside to outside the PLTs. The PAC-1 binding level in the PRT-treated PLTs significantly increased from $36.2 \pm 19.2\%$ to $95.6 \pm 2.8\%$ whereas that in the control PLTs also increased from $8.5 \pm 6.5\%$ to $66.9 \pm 22.7\%$ (Fig. 4A). The retention rate in the PRT-treated PLTs significantly increased from $54.3 \pm 16.5\%$ to $88.5 \pm 15.6\%$ whereas that in the control PLTs increased from $31.3 \pm 7.7\%$ to $82.5 \pm 12.3\%$ (Fig. 4B). As is the case for the Day 1 PRT-treated PLTs, there were many PLTs and large thrombi adhering to multiple beads through which the PRT-treated PLTs and control PLTs passed after the addition of Mn^{2+} (Fig. 4C). These findings suggest that thrombus formation on collagen was restored owing to the reactivation of α Ib β 3 in the PRT-treated PLTs after the addition of Mn^{2+} .

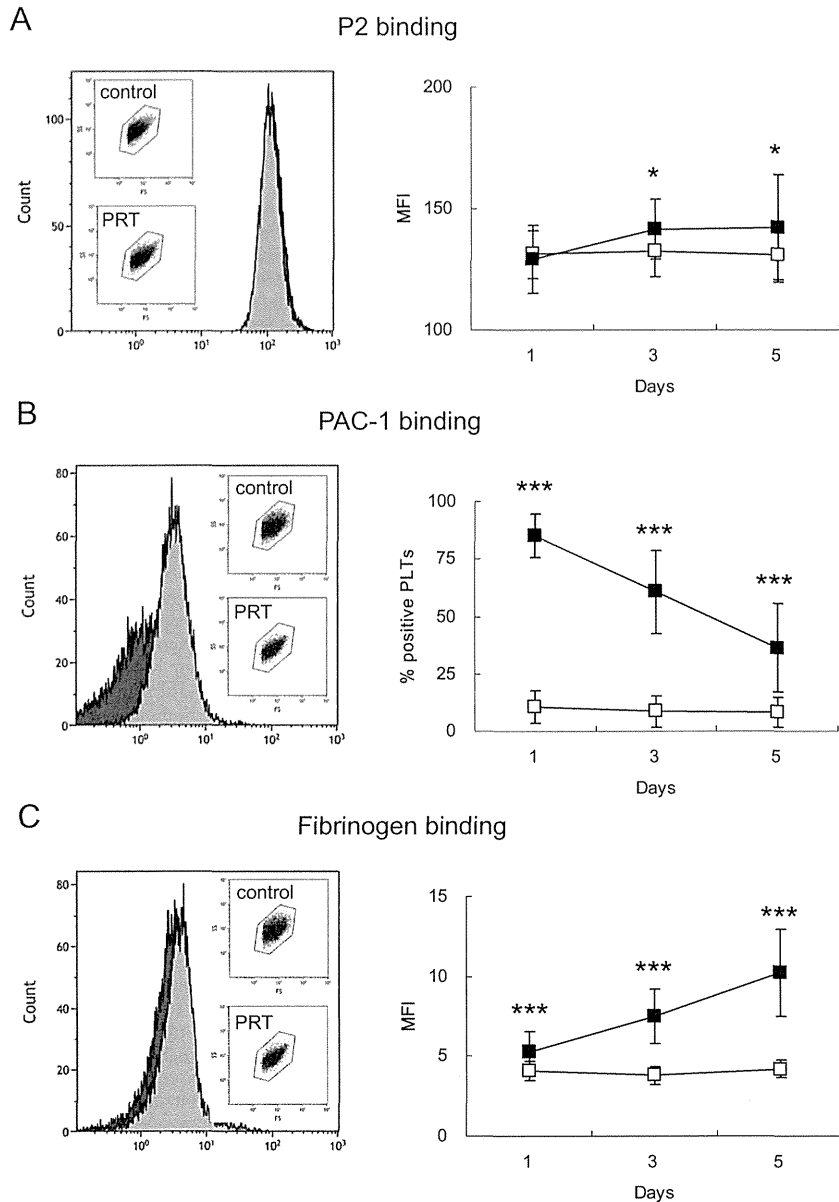


Fig. 3. Effects of PRT treatment on α IIb β 3 level and fibrinogen binding as determined by flow cytometry. (A) Total α IIb β 3 level represented as CD41 positivity; (B) activated α IIb β 3 represented as PAC-1 binding; (C) fibrinogen binding. Figure 3C shows representative results obtained using the fibrinogen-specific antibody PF056, but the same results were obtained using the other antibodies specific for fibrinogen (IMS09-038-355). Representative histograms (left column) indicate P2, PAC-1, and fibrinogen binding on the Day 1 control (■) and the Day 1 PRT-treated (□) PLTs. Boxes in each graph (right column) indicate the values for the control (□) and the PRT-treated (■) PLTs presented as mean \pm SD. (Insets in histograms) Dot plots of forward scatter versus side scatter of a typical sample, with the gate set to exclude small vesicles and large aggregates. $n = 17$ (□); $n = 32$ (■). MFI = mean fluorescence intensity. * $p < 0.05$; *** $p < 0.001$.

TABLE 1. Correlation between retention rates and the flow cytometer variables

Variable	r	p value
P2 binding (MFI)	0.067	0.420
PAC-1 binding (% positive PLTs)	0.840	<0.001
Fibrinogen binding (MFI)	0.234	0.004

MFI = mean fluorescence intensity; r = Spearman's rank correlation coefficient.

DISCUSSION

With the aim of clarifying the effects of PRT treatment on thrombus formation in PLTs, we performed a thrombus formation assay using the collagen column method. This method was designed to assess PLT function in terms of thrombus formation under nearly physiologic conditions rather than turbidometric aggregometry, in which PLTs are stimulated by agonists under stirring condition. The collagen column method had also been used in a clinical setting for the evaluation of dose dependency of anti-PLT agent.¹⁷ We found that thrombus formation in the PRT-treated PLTs was enhanced under flow in the collagen column. The enhanced thrombus formation was well sustained during the storage period. The finding of sustained thrombus formation after storage was in agreement with those of *in vitro* experiments using Impact-R and aorta segments. However, the thrombus formation ability was the highest immediately after the PRT treatment in the collagen column method, which was clearly different from those in the other two experiments. Using Impact-R, the surface coverage by aggregates of the PRT-treated PLTs on the day after PRT treatment was higher than that of the control PLTs, but there was no significant difference in the average size of aggregates between them.¹⁰ In the experiments using rabbit aorta segments, the adhesive and cohesive functions of the PRT-treated PLTs were higher on Day 5 but lower on the day of PRT treatment compared with those of the control PLTs.¹¹ Thus, the evaluation of the ability of thrombus formation of PRT-treated PLTs may differ depending on the assay system used, and this awaits careful observation in clinical studies.

We considered that α Ib β 3 is involved in the enhancement of thrombus formation in the PRT-treated PLTs. The Mirasol PRT system uses UV radiation in a wide range of wavelengths from UV-A to UV-C (265 to 370 nm).^{12,21} Verhaar and colleagues²² reported that UV-C (254 nm) breaks disulfide bonds of α Ib β 3 and causes conformational changes of α Ib β 3, which leads to the enhancement of fibrinogen binding. Zhi and coworkers²³ suggested that UV-B (290 to 320 nm) also activates α Ib β 3 and enhances fibrinogen binding and that protein kinase C is involved in α Ib β 3 activation. Whereas they examined the effects of UV radiation alone, we showed in this study that the Mirasol PRT system, which uses a photosensitizer as well,

also induced the marked activation of α Ib β 3 and enhanced fibrinogen binding. Interestingly, α Ib β 3 activated by PRT treatment did not bind fibrinogen completely immediately after the treatment. Although the level of α Ib β 3 activation induced by PRT treatment decreased with storage time, the level of fibrinogen binding on PLTs slightly increased, indicating that the activation state of α Ib β 3 represented as PAC-1 binding did not correlate with fibrinogen binding.

We speculate that, although slight conformational changes recognized by the PAC-1 antibody occurred, α Ib β 3 activation induced by PRT treatment did not cause sufficient conformational changes for α Ib β 3 to bind fibrinogen, which presents a distinct status from α Ib β 3 activation induced by physiologic agonists such as thrombin.²⁴ Takagi and colleagues²⁵ reported that integrins exist in at least three conformational states depending on the activation level: a bent conformer, an extended conformer with a closed headpiece, and an extended conformer with an open headpiece. Bunch²⁶ suggested that the conformational change of α Ib β 3 needs an increase in both affinity and avidity to strongly bind fibrinogen. It is thus possible that α Ib β 3 activation induced by PRT treatment is only partial so that a proportion of α Ib β 3 molecules on the PLT surface may bind fibrinogen or those molecules may weakly bind fibrinogen. The reason why the level of fibrinogen binding onto α Ib β 3 increased during storage was unclear. There may be effects of intrinsic activation of α Ib β 3 associated with the PLT storage lesion.

We found a strong correlation between thrombus formation assayed by the collagen column method and α Ib β 3 activation represented as PAC-1 binding. There was no correlation between thrombus formation and total α Ib β 3 level represented as CD41 positivity or fibrinogen binding. It is thus possible that the conformational changes of α Ib β 3 caused by PRT treatment enhanced the thrombus formation on collagen-coated beads. Jackson²⁷ reported that the contact of PLTs with collagen or the von Willebrand factor under various flow conditions activates α Ib β 3 and promotes thrombus growth. It seems that α Ib β 3 rapidly shifts from being partially activated to fully activated when the PRT-treated PLTs come into contact under flow with the collagen on the beads, leading to the enhanced thrombus formation. The thrombus formation assay by the collagen column method seemed to reflect the activation state of α Ib β 3 in PRT-treated PLTs quite well.

Both the thrombus formation and the PAC-1 binding to α Ib β 3 on the PRT-treated PLTs were reduced on Day 5. When Mn²⁺ was added to the PLTs, the α Ib β 3 on the PRT-treated PLTs as well as that in the control PLTs was activated, resulting in the restoration of thrombus formation. Mn²⁺ directly and fully activates α Ib β 3 without being mediated by inside-out signals from within the PLTs and enables the binding of α Ib β 3 to fibrinogen and

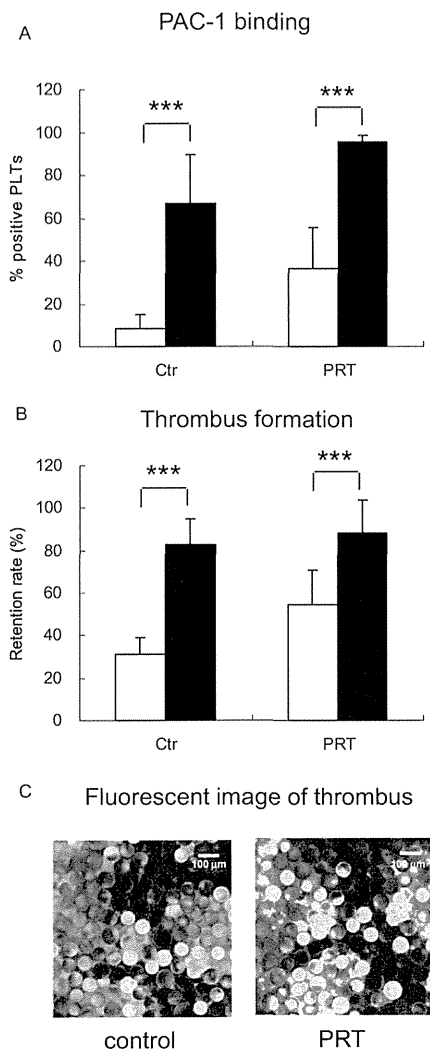


Fig. 4. Effects of Mn²⁺ on α IIb β 3 activation and thrombus formation. (A) Activated α IIb β 3 represented as PAC-1 binding on Day 5 control PLTs (Ctrl, n = 7) and Day 5 PRT-treated PLTs (PRT, n = 24) in the presence (■) or absence (□) of Mn²⁺. (B) Enhancement of thrombus formation determined by collagen column method in Day 5 control PLTs (Ctrl, n = 7) and Day 5 PRT-treated PLTs (PRT, n = 24) in the presence (■) or absence (□) of Mn²⁺. (C) Typical fluorescent image of thrombus on collagen-coated beads through which Day 5 PLTs incubated with Mn²⁺ passed: (left) control, (right) PRT-treated. Thrombus formation was determined on the basis of retention rate (%) presented as mean \pm SD. ***p < 0.001.

fibrin.^{19,28,29} The result showed a sufficient potential of reactivation of Day 5 PRT-treated PLTs in terms of α IIb β 3 activation and the restoration of thrombus formation in the column, suggesting that the functions of α IIb β 3 are not impaired. After immediate activation by PRT treatment, the α IIb β 3 in the PRT-treated PLTs gradually returned to the status with lower-level activation during storage. However, it was intriguing that the activation state lasted as long as 5 days with decreasing trend that seemed reversible.^{30,31} Although we could not find an explanation for this reversible and long-lasting α IIb β 3 activation, it may be related to the activation state of α IIb β 3 that did not bind fibrinogen.^{26,32}

In this study, thrombus formation ability was measured by the collagen column method as an index of PLT function. In the collagen column method, however, only the reaction between PLTs and collagen, the major component of the subendothelium, was evaluated in the absence of RBCs. The reaction between PLTs and collagen is important for evaluating the PLT function in the initial phase of thrombus formation. However, how much this reaction contributes to the complicated *in vivo* thrombus formation process has not been fully clarified yet. In addition, how the insufficient α IIb β 3 activation in PRT-treated PLTs leads to the enhancement of thrombus formation on collagen is unclear in our study. However, it has been reported that the signaling from the collagen receptor regulates α IIb β 3 activation and the subsequent thrombus formation.³³ We consider that there is a close relationship between the enhancement of thrombus formation and insufficient α IIb β 3 activation.

Although our results show the increased and sustained capacity of binding of PRT-treated PLTs to collagen, they indicate a possibility of unwanted binding of treated PLTs to undamaged endothelial cells under physiologic conditions. Although we do not have any expectation on this issue with our current system, we are currently developing an aggregometric system that could evaluate PLT aggregation caused by shear stress in the absence of collagen.

In conclusion, our studies using the collagen column method indicated that PRT treatment enhanced the thrombus formation on collagen and that the ability of the thrombus formation was well maintained during the storage period. We consider that the sustained α IIb β 3 activation is related to the enhancement of thrombus formation. In the absence of the contact of PLTs with collagen, however, α IIb β 3 activation induced by PRT treatment may be only partial. Upon contact with collagen, thrombus is formed completely along with the reactivation of α IIb β 3. These results could have an implication in the clinical setting of PLT transfusion in that the modifications of surface glycoproteins on PLTs caused by PRT treatment might not significantly affect the hemostatic effects of PRT-treated PLTs when transfused. Ultimately, the clinical

impacts of these findings on the hemostatic or even thrombogenic potential of PRT-treated PLTs should be evaluated in appropriate clinical trials.

ACKNOWLEDGMENT


The authors thank the Japanese Red Cross Tokyo Metropolitan Blood Center for providing processed blood PLTs for this study.

CONFLICT OF INTEREST

The disposables and the instrumentation for conducting pathogen reduction by the Mirasol system were provided without charge by Terumo BCT. Otherwise, none of the authors of this article have any conflicts of interest to report as defined by AABB's policy.

REFERENCES

- Blajchman MA, Goldman M, Baeza F. Improving the bacteriological safety of platelet transfusion. *Transfus Med Rev* 2004;18:11-24.
- Solheim BG, Seghatchian J. The six questions of pathogen reduction technology: an overview of current opinions. *Transfus Apher Sci* 2008;39:51-7.
- Kumar V, Lockerbie O, Keil SD, et al. Riboflavin and UV-light based pathogen reduction: extent and consequence of DNA damage at the molecular level. *Photochem Photobiol* 2004;80:15-21.
- Goodrich RP, Edrich RA, Li J, et al. The Mirasol PRT system for pathogen reduction of platelets and plasma: an overview of current status and future trends. *Transfus Apher Sci* 2006;35:5-17.
- Hervig T, Seghatchian J, Apelseth TO. Current debate on pathogen inactivation of platelet concentrates—to use or not to use? *Transfus Apher Sci* 2010;43:411-4.
- Picker SM, Steisel A, Gathof BS. Effects of Mirasol PRT treatment on storage lesion development in plasma-stored apheresis-derived platelets compared to untreated and irradiated units. *Transfusion* 2008;48:1685-92.
- Li J, Lockerbie O, de Korte D, et al. Evaluation of platelet mitochondria integrity after treatment with Mirasol pathogen reduction technology. *Transfusion* 2005;45:920-6.
- Picker SM, Steisel A, Gathof BS. Cell integrity and mitochondrial function after Mirasol-PRT treatment for pathogen reduction of apheresis-derived platelets: results of a three-arm in vitro study. *Transfus Apher Sci* 2009;40:79-85.
- Picker SM, Oustianskaia L, Schneider V, et al. Functional characteristics of apheresis-derived platelets treated with ultraviolet light combined with either amotosalen-HCl (S-59) or riboflavin (vitamin B₂) for pathogen-reduction. *Vox Sang* 2009;97:26-33.
- Picker SM, Schneider V, Gathof BS. Platelet function assessed by shear-induced deposition of split triple-dose apheresis concentrates treated with pathogen reduction technologies. *Transfusion* 2009;49:1224-32.
- Perez-Pujol S, Tonda R, Lozano M, et al. Effects of a new pathogen-reduction technology (Mirasol PRT) on functional aspects of platelet concentrates. *Transfusion* 2005;45:911-9.
- AuBuchon JP, Herschel L, Roger J, et al. Efficacy of apheresis platelets treated with riboflavin and ultraviolet light for pathogen reduction. *Transfusion* 2005;45:1335-41.
- Cazenave JP, Folléa G, Bardiaux L, et al. A randomized controlled clinical trial evaluating the performance and safety of platelets treated with MIRASOL pathogen reduction technology. *Transfusion* 2011;50:2362-75.
- Johansson PI, Simonsen AC, Brown PN, et al. A pilot study to assess the hemostatic function of pathogen-reduced platelets in patients with thrombocytopenia. *Transfusion* 2013;53:2043-52.
- Schubert P, Culibrk B, Coupland D, et al. Riboflavin and ultraviolet light treatment potentiates vasodilator-stimulated phosphoprotein Ser-239 phosphorylation in platelet concentrates during storage. *Transfusion* 2012;52:397-408.
- Polanowska-Grabowska R, Gear AR. High-speed platelet adhesion under conditions of rapid flow. *Proc Natl Acad Sci U S A* 1992;89:5754-58.
- Polanowska-Grabowska R, Gear AR. Role of cyclic nucleotides in rapid platelet adhesion to collagen. *Blood* 1994;83:2508-15.
- Litvinov RI, Nagaswami C, Vilaire G, et al. Functional and structural correlations of individual α Ib β 3 molecules. *Blood* 2004;104:3979-85.
- Blue R, Li J, Steinberger J, et al. Effects of limiting extension at the α IIb β 3 gene on ligand binding to integrin α Ib β 3. *J Biol Chem* 2010;285:17604-13.
- Colton T. *Statistics in medicine*. Boston (MA): Little, Brown and Company; 1974.
- Ruane PH, Edrich R, Gampp D, et al. Photochemical inactivation of selected viruses and bacteria in platelet concentrates using riboflavin and light. *Transfusion* 2004;44:877-85.
- Verhaar R, Dekkers DW, De Cuyper IM, et al. UV-C irradiation disrupts platelet surface disulfide bonds and activates the platelet integrin α IIb β 3. *Blood* 2008;112:4935-9.
- Zhi L, Chi X, Gelderman MP, et al. Activation of platelet protein kinase C by ultraviolet light B mediates platelet transfusion-related acute lung injury in a two-event animal model. *Transfusion* 2013;53:722-31.
- Malaver E, Romaniuk MA, D'Atri LP, et al. NF-kappaB inhibitors impair platelet activation responses. *J Thromb Haemost* 2009;7:1333-43.
- Takagi J, Petre BM, Walz T, et al. Global conformational rearrangements in integrin extracellular domains in outside-in and inside-out signaling. *Cell* 2002;110:599-611.
- Bunch TA. Integrin α IIb β 3 activation in Chinese hamster ovary cells and platelets increases clustering rather than affinity. *J Biol Chem* 2010;285:1841-9.

27. Jackson SP. The growing complexity of platelet aggregation. *Blood* 2007;109:5087-95.
28. Haling JR, Monkley SJ, Critchley DR, et al. Talin-dependent integrin activation is required for fibrin clot retraction by platelets. *Blood* 2011;117:1719-22.
29. Zhang G, Xiang B, Ye S, et al. Distinct roles for Rap1b protein in platelet secretion and integrin α Ib β 3 outside-in signaling. *J Biol Chem* 2011;286:39466-77.
30. Kamae T, Shiraga M, Kashiwagi H, et al. Critical role of ADP interaction with P2Y₁₂ receptor in the maintenance of alpha(IIb)beta3 activation: association with Rap1B activation. *J Thromb Haemost* 2006;4:1379-87.
31. Tadokoro S, Nakazawa T, Kamae T, et al. A potential role for α -actinin in inside-out α Ib β 3 signaling. *Blood* 2011; 117:250-8.
32. Kamata T, Handa M, Ito S, et al. Structural requirements for activation in alphaIIb beta3 integrin. *J Biol Chem* 2010; 285:38428-37.
33. Arthur JF, Qiao J, Shen Y, et al. ITAM receptor-mediated generation of reactive oxygen species in human platelets occurs via Syk-dependent and Syk-independent pathways. *J Thromb Haemost* 2013;10:1133-41. 

Cytomegalovirus (CMV) seroprevalence in Japanese blood donors and high detection frequency of CMV DNA in elderly donors

Yasumi Furui,¹ Masahiro Satake,² Yuji Hoshi,² Shigeharu Uchida,² Ko Suzuki,³ and Kenji Tadokoro^{1,2}

BACKGROUND: The current prevalence of cytomegalovirus (CMV) in Japan and the risk of CMV transfusion transmission are unknown in the era of seronegative leukoreduced blood components.

STUDY DESIGN AND METHODS: We measured CMV-specific immunoglobulin (Ig)M and IgG in 2400 samples of whole blood collected from 12 groups of blood donors categorized by sex and age at 10-year intervals from their teens to their 60s. We also tested for CMV DNA using polymerase chain reaction in the cellular fractions of all samples.

RESULTS: We found that 76.6% of blood donors were CMV seropositive. The seroprevalences among donors in their 20s and 30s were 58.3 and 73.3%, respectively. We detected CMV DNA in the cellular fraction of 4.3% of samples from donors in their 60s and in 1.0% of samples from donors younger than 60 years. None of the 562 seronegative samples was DNA positive. Furthermore, 14% of DNA-positive samples also contained DNA in the plasma fraction, and two of five such samples were derived from donors in their 60s.

Leukoreduced plasma components derived from donations with CMV DNA in plasma samples also contained a relevant amount of CMV DNA.

CONCLUSION: The seroprevalence of CMV among Japanese blood donors of child-bearing age has not changed over the past 15 years. Latent CMV becomes reactivated more frequently among elderly donors than among younger donors. A proportion of them have free CMV DNA in their plasma fraction, which could not be diminished by leukoreduction. The risk of transfusion-transmitted CMV infection in blood with plasma CMV DNA should be determined.

Human cytomegalovirus (CMV; *Human herpesvirus 5*) ubiquitously infects humans and persists in a latent form for long periods. It can cause asymptomatic infection in the general population or a mononucleosis-like syndrome or transient hepatitis in some healthy individuals. However, it can cause serious morbidity and mortality in immunocompromised hosts, and congenital or perinatal CMV infection causes developmental abnormalities in newborns. Morbidity can arise due to either primary infection or CMV reactivation. The transfusion of blood contaminated with CMV could be a source of primary infection in seronegative patients. Thus, CMV-safe blood components are typically required for transfusing seronegative patients who will undergo marrow or organ transplantation, patients with immunodeficiency syndrome, or premature infants. Blood facilities have implemented serologic screening of donated blood for CMV-specific immunoglobulin (Ig)G to mitigate the incidence of transfusion-transmitted CMV infection (TT-CMV) in such patients. This is conducted universally or in response to requests from physicians and has largely prevented TT-CMV infection.¹

Leukoreduction using white blood cell (WBC) filters has been widely implemented in blood facilities to help reduce the side effects of residual WBCs in blood components such as febrile reactions or alloimmunization against WBC antigen. Leukoreduction under good

ABBREVIATION: TT-CMV = transfusion-transmitted cytomegalovirus infection.

From the ¹Blood Service Headquarters and the ²Central Blood Institute, Japanese Red Cross, Tokyo; and the ³Japanese Red Cross Tohoku Block Blood Center, Sendai, Japan.

Address correspondence to: Masahiro Satake, MD, Japanese Red Cross Central Blood Institute, 2-1-67, Tatsumi, Koto-ku, Tokyo 135-8521, Japan; e-mail: m-satake@jrc.or.jp.

Received for publication May 23, 2013; revision received July 18, 2013, and accepted July 20, 2013.

doi: 10.1111/trf.12390

TRANSFUSION 2013;53:2190-2197.

manufacturing practices could also abrogate the transmission of WBC-associated virus such as CMV, Epstein-Barr virus, or human T cell leukemia virus. Thus, leukoreduced blood components have been advocated as an alternative to transfusion for patients at risk for CMV when seronegative blood is unavailable, although whether leukoreduced blood is as safe as seronegative blood in terms of TT-CMV risk remains a matter of debate.²⁻⁵

Breakthrough cases have been attributed to transfusion with CMV-seronegative, but CMV DNA-positive blood that might have been donated during a window period, namely, the preseroconversion viremic phase of acute infection.⁶ This could justify using leukoreduced blood to avoid transfusion with blood obtained during window periods that serologic screening could miss.⁷ Thus, seronegative leukoreduced blood components are currently regarded as the safest strategy to prevent TT-CMV. However, Ziemann and colleagues⁸ recently reported that up to 2.9% of plasma derived from donors during the window period contains CMV DNA. Because leukofiltration might not efficiently remove free CMV from the plasma fraction, this would pose another TT-CMV risk that could not be overcome by combining the two strategies.

We screened blood samples (n = 2400) donated equally by male and female volunteers of all age categories using serologic assays and nucleic acid amplification testing (NAT) to assess the risk of CMV transmission in Japan, particularly through transfusion with leukoreduced and seronegative blood components. We established a national prevalence and demographic trend for CMV infection over a range of donor ages and found no blood samples that were both viremic and seronegative. We also found that the frequency of CMV DNA positivity was higher in samples from elderly than from younger donors.

MATERIALS AND METHODS

Blood samples

We sequentially selected whole blood samples at the Japanese Red Cross Tokyo Blood Center in November 2010, where whole blood and blood samples were collected from five prefectures around the greater Tokyo metropolitan area. The samples were allocated to 12 groups according to donor sex and age at 10-year intervals from the 20s to the 60s and from age 16 to 19 years. Each of the 12 categories comprised 200 blood samples. Whole blood collected into tubes containing ethylenediaminetetraacetic acid was separated by centrifugation, during which the separation media rose to the interface between the plasma and the cellular fraction and formed a hard gel. We could thus keep them frozen until use without the two fractions becoming mixed. The plasma fraction was analyzed by CMV serology and CMV NAT. After removing the remaining plasma and interface gel, the top portion of the

cellular fraction was suspended in the same volume of phosphate-buffered saline for DNA extraction.

CMV serology assays

We tested CMV-specific IgG and IgM antibodies using automated microparticle enzyme immunoassays (EIAs) and an immunochemical automated analyzer (AxSYM CMV-G and CMV-M, Abbott Laboratories, Abbott Japan, Tokyo, Japan).

DNA extraction

We extracted DNA from the cellular fraction of blood samples using the automated DNA purification kits (QIAAsymphony SP and QIAAsymphony DNA Midi kits, Qiagen, Tokyo, Japan) according to the protocol provided by the manufacturer (DNA Blood 1000). The input and output sample volumes were 1200 and 200 μ L, respectively. Plasma DNA was likewise extracted from samples that were positive for DNA in the cellular fraction using a virus and bacteria detection kit (QIAAsymphony Midi kit, Qiagen) with its accompanying protocol (Virus Cellfree 1000). The input and output sample volumes were 1.0 mL and 60 μ L, respectively.

CMV NAT

We detected CMV DNA using TaqMan PCR and a sequence detection system (ABI PRISM7900HT, Applied Biosystems, Tokyo, Japan) and artus CMV TM PCR kits (Qiagen) according to the manufacturer's instructions.

We also prepared an in-house TaqMan PCR to detect CMV DNA. This system amplifies a 58-bp fragment of the UL83 gene that encodes phosphorylated 65-kDa proteins (pp65). The forward and reverse primers were 5'-TGCC ATACGCCTTCCAATTC-3' and 5'-TGGCTACGGTTCAG GGTC-3', respectively. The TaqMan probe, 5'-CGGT AGATGTCGTTGGC-3', was labeled with a reporter dye (6-carboxyfluorescein, FAM) at the 5' end and a minor groove binder at the 3' end. The amplification reagent was supplied with a probe PCR kit (QuantiTect, Qiagen). Each reaction mixture comprised 30 μ L of master mix and 20 μ L of extracted DNA (equivalent to 120 μ L of original sample). The thermocycling protocol comprised 50°C for 2 minutes and 95°C for 10 minutes, followed by 40 cycles of 95°C for 15 seconds and 60°C for 60 seconds. The nucleic acid concentration was calculated by measuring the absorbance of the extracted DNA at 260 nm.

A validation study for PCR sensitivity included NATrol NATCMV-0004 (ZeptoMetrix, Buffalo, NY) as the external reference CMV for both PCR analyses. The reference solution was serially diluted in 5% bovine serum albumin (BSA) and portioned into small tubes for PCR analysis over a period of 4 days. We tested CMV concentrations five times daily for each PCR procedure, for a total

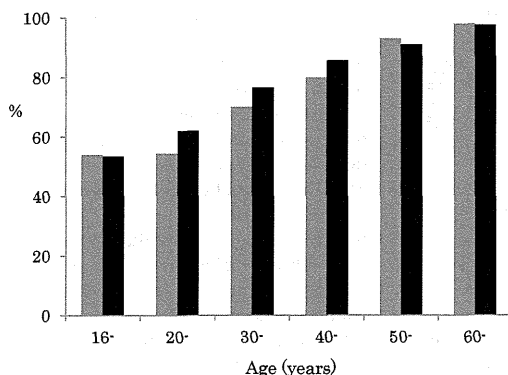


Fig. 1. Age distribution of CMV-specific IgG prevalences in (■) men and (■) women.

of 20 replicates at each concentration. We then calculated the 95 and 50% limits of detection for each PCR using probit analysis. Correlation study between the reference solution and first World Health Organization international standard (NIBSC 09/162) revealed that 32.3 genome equivalents/mL (geq/mL) was equivalent to 1 IU/mL. Samples in which the PCR results were ambiguous were further analyzed using nested PCR targeting the UL139 sequence as described by Bradley and colleagues⁹ with the modification for DNA polymerase (KAPA DNA polymerase, Nippon Genetics, Tokyo, Japan).

To adjust the amount of CMV DNA for the number of WBCs in the sample, we estimated the number of Exon 5 sequences of CD81 in specimens using real-time PCR.¹⁰ CD81 was chosen as a marker of WBCs as it is present with two haploids in a cell. Amounts of CMV DNA are described as geq per 6.0×10^6 WBCs (geq/PBL unit) in this study. The lowest limit of quantitative CMV DNA detection was 40 geq/mL before adjustment for WBC numbers.

Statistical analysis

Data were analyzed using computer software (SSRI, Excel Statistics, Version 8, Social Survey Research Information, Tokyo, Japan; for Windows, Microsoft Excel 2007, Tokyo, Japan). Significance was determined using the chi-square test and t test. *p* values of less than 0.05 were considered significant.

RESULTS

We initially examined the prevalence of anti-CMV among Japanese blood donors. Figure 1 shows the prevalence of specific IgG among the age categories. The prevalence exceeded 50% even in male and female teenagers and steadily increased over time to reach nearly 100% in their

60s. Although not significant, the prevalence tended to be higher in females than in males aged from the 20s to the 40s. The increase in the prevalence was the highest between the 20s and 30s (15%; combined for both sexes) and gradually decreased with age to 5.8% between the 50s and 60s. The mean prevalence in the six age categories was 76.3%. The overall CMV prevalence adjusted for an assumed population with the age distribution of Japanese blood donors (Japanese Red Cross data, 2010) was 76.6%. The IgM prevalence was higher among females than males between the ages of 16 and 39 years ($p < 0.05$, Table 1). Seven donors were IgM positive and IgG negative, and four of them were teenagers.

We next examined the presence of CMV DNA in the cellular fraction of 2400 whole blood samples. A validation study showed that the 95 and 50% limits of CMV DNA detection for artus CMV TM PCR were 41.6 and 5.3 geq/mL, respectively, and those for the in-house PCR were 29.6 and 5.4 geq/mL, respectively (Table 2). Only samples that were positive for at least two PCR analyses including nested PCR targeting the UL139 sequence were defined as CMV DNA positive. We identified 37 samples that were positive for CMV DNA in the cellular fraction (Table 3). Four other samples were positive for only one PCR analysis and were defined as DNA indeterminate. Table 4 shows the relationship between DNA positivity and the serostatus of the specific antibody. We found DNA positivity in six (6.6%) of 91 samples that were both IgM and IgG positive and in 31 (1.8%) of 1740 that were only IgG positive. Although the samples that were positive only for IgM did not contain any that were DNA positive, the frequency of DNA positivity was significantly higher in six (6.12%) of 98 samples that were IgM positive with or without IgG than in those that were positive only for IgG ($p < 0.03$). Viral load was significantly higher in CMV DNA-positive samples that were both IgM and IgG positive (mean, 670 geq/PBL unit) than in those that were only IgG positive (170 geq/PBL unit, $p < 0.03$, t test). Notably, none of the 562 samples that were both IgM and IgG negative was also DNA positive.

Table 5 compares the distribution of 37 DNA-positive samples with age categories. The frequency of DNA positivity was significantly higher (17/400, 4.3%) among donors in their 60s than in any other age category (0.8%-1.3%, $p < 0.03$) from the teens to the 50s or the combined age category (1.0%, $p < 0.03$) from 16 to 59 years. The range of viral load in the 37 DNA-positive samples was between less than 40 and 3.4×10^3 geq/PBL unit (mean, 250 geq/PBL unit; median, 80 geq/PBL unit). The difference in viral load in the samples between donors aged less than 60 years (mean, 310 geq/PBL unit) and those in their 60s (mean, 170 geq/PBL unit) was not significant. The presence of DNA in the plasma fraction was further investigated in these 37 samples. Five (13.5%) of them were plasma DNA positive with a viral load between less than

TABLE 1. Prevalence of CMV-specific IgM among blood donors*

Age (years)	Male		Female		Total	
	Positivity	Percent	Positivity	Percent	Positivity	Percent
16-19	6	3.0†	13 (4)	6.5†	19 (4)	4.8
20-29	5 (1)	2.5†	15	7.5†	20 (1)	5.0
30-39	5 (1)	2.5†	13	6.5†	18 (1)	4.5
40-49	8	4.0	10	5.0	18	4.5
50-59	5 (1)	2.5	3	1.5	8 (1)	2.0
60-69	6	3.0	9	4.5	15	3.8
Total	35 (3)	2.9	63 (4)	5.3	98 (7)	4.1

* Numbers of donors positive only for specific IgM are shown in parentheses.

† IgM prevalence significantly higher among female donors than among male donors (16-19, 20-29, and 30-39 years); chi-square test ($p < 0.05$).

40 and 5.8×10^3 geq/mL (median, 170 geq/mL). These five were scattered across age categories with two being in their 60s. One sample obtained from a teenaged donor was IgM and IgG positive and the other four were positive only for IgG. We identified two more samples from donors in their 60s that were DNA positive with only one PCR analysis.

We interdicted three components of fresh-frozen plasma that had CMV DNA in the plasma fraction. All of them were derived from whole blood that was leukoreduced before storage. We also detected CMV DNA in all three plasma components. One component donated by the IgM- and IgG-positive teenaged male donor contained 9.7×10^3 geq/mL CMV DNA and the other two components that were positive only for IgG from donors in their 60s contained 1.9×10^2 and 1.6×10^3 geq/mL CMV DNA.

DISCUSSION

We investigated the prevalence of CMV among Japanese blood donors categorized by sex and age at 10-year intervals. The more than 50% prevalence of CMV infection among individuals aged between 16 and 19 years is in contrast with the approximately 30%¹¹ prevalence in other developed countries. The increase in the prevalence (15%) between donors aged in their 20s and 30s implies that young adults become infected with CMV at a rate of 1.5% per annum. This is similar to the annual rate of 1.69% observed between 1994 and 1999,¹² implying that the risk of CMV infection among females of child-bearing age that is directly related to symptomatic fetal CMV infection has not changed over the past 15 years. The reason for the sustained high prevalence in Japan is unclear, but prolonged breast-feeding and communal child care practices in Japan probably influenced the rates in younger donors. The prevalence in Japan has become almost maximal after the age of 60 years, which contrasts with the continuous lifelong primary infection found in other developed countries.¹¹ The CMV seroconversion rate (1.33%)¹¹ among German blood donors aged 30 to 35 years is close to

the 1.5% rate of increase described above. However, care must be taken in comparing the present results with those of the German study because our results were generated from a cross-sectional study whereas the German findings were obtained through longitudinal follow-up of seronegative donors. Although insignificant, the prevalence in females tended to increase sooner than in males, a finding that is consistent with the higher prevalence of specific IgM in younger females than in younger males.^{13,14}

We detected CMV DNA in the cellular fraction of 1.7% (41/2400) of all, or 2.2% (41/1831) of the seropositive, samples with or without specific IgM. This frequency was comparable to those reported by Greenlee and colleagues¹⁵ and Roback and colleagues.¹⁶ We found CMV DNA more frequently in samples that were IgM positive than in those that were only IgG positive (6.12% vs. 2.0%, $p < 0.03$), indicating that active CMV replication occurs more frequently during acute primary infection that is often accompanied by IgM positivity. None of the samples from the group of seven donors that was positive only for IgM was CMV DNA positive. This is reasonable because Ziemann and coworkers¹⁷ detected CMV DNA only in 10% of 148 primary seroconverted blood donors. At that rate we would be unable to identify a single DNA-positive individual in our study population. The same authors showed that CMV DNA levels peak during the late phase of primary infection in newly seropositive donors.⁸ Although whether a rationale exists for introducing screening for specific IgM in addition to IgG remains to be determined,¹⁸ the chemiluminescence tests for CMV currently applied by the Japanese Red Cross detect only IgG. Although we have discussed seroprevalence and its relationship with the presence of DNA by interpreting IgM positivity as representing primary infection, reactivity for CMV-specific IgM measured by EIAs must be considered with caution. Several articles have reported frequent non-specific reactions^{19,20} and suggest including Western blot analyses or IgG avidity assays to ensure reactivity. Because of the small plasma volume of most of the donor samples, we were unable to apply these analyses. Thus, the above findings and our interpretations based on categories by IgM positivity might be inconclusive and require further investigation.

We found no DNA-positive samples among 562 that were seronegative, suggesting that the likelihood of donating DNA-positive blood during the window period⁷ is very low in Japan. This finding is similar to that described by Roback and coworkers,¹⁶ who found no CMV DNA positivity among 514 healthy, seronegative blood donors. However, these findings do not allow underestimation of